Microscopic and Macroscopic Magnetoelastic Tensors for the Rare-Earth Garnets from Electron Paramagnetic Resonance under Pressure*

T. G. PHILLIPS† AND R. L. WHITE
Stanford Electronics Laboratories, Stanford University, Stanford, California
(Received 20 March 1967)

The local microscopic magnetoelastic tensors have been determined for Gd^{3+}, Yb^{3+}, and Er^{3+} in diamagnetic garnet hosts, the theory connecting these microscopic magnetoelastic tensors with the macroscopic magnetostriction constants of the magnetically ordered rare earth has been developed, and predictions made for the magnetostriction constants λ_{100} and λ_{111} of Gd, Yb, and Er iron garnets. Because the local site symmetry for the rare-earth ion in the garnets is low (orthorhombic), the number of independent constants in the microscopic magnetoelastic tensor is large. The magnetoelastic tensor has therefore been examined for "hidden" symmetries implied by the physical mechanisms underlying the magnetoelastic energy. The tensor was found generally not to be symmetric across the diagonal, whether the dominant physical effect was a change in crystal-field energy or a change in effective g factor of the ion involved. The consequences of invariance of the trace of the crystal-field energy matrix or of the $\mathbf{g}$ tensor were examined. After analytic machinery involving the transformation of the local site tensors to the crystal-field axes was developed, the microwave EPR spectra of Gd^{3+}, Yb^{3+}, and Er^{3+} in garnet hosts under uniaxial pressure were analyzed to yield the full orthorhombic magnetoelastic tensor for each ion. The connection between the single-ion rare-earth magnetoelastic tensors and the magnetostriction constants of the cubic ordered magnetic rare-earth iron garnets was then derived using a molecular-field model and a single-ion Hamiltonian. The magnetostriction constants λ_{100} and λ_{111} for GdIG, YbIG, and ErIG (in units of 10^{-6}) were predicted to be 4.2 and 1.7, 82 and 34, and 216 and -282, respectively. These are all within a factor of 2 of the observed low-temperature magnetostriction constants, except for λ_{111} for YbIG, which is of the correct magnitude but the wrong sign. The origin of this discrepancy is presumed to be in the neglect of the change of the molecular field with strain.

1. INTRODUCTION

A PARAMAGNETIC ion incorporated dilutely into a diamagnetic host displays an energy-level scheme which is sensitive to the crystal-field environment of the site and to the crystallographic orientation of an applied magnetic field. The behavior of the low-lying levels of the ion can often be described by a "spin Hamiltonian" which treats the low-lying levels as an isolated manifold and which is valid to the degree that the states spanning the manifold remain unmixed with external states under the perturbations contemplated. The spin Hamiltonian has the point symmetry of the site involved; if there are several crystallographically equivalent but magnetically inequivalent sites per unit cell, their spin Hamiltonians are related by the same symmetry operations of the crystal space group which take the inequivalent sites into one another. The parameters entering the spin Hamiltonian can generally be determined from electron-paramagnetic-resonance (EPR) experiments. If one subjects the host crystal to stresses, the induced deformations alter the crystal-field environment of the paramagnetic ion and consequently alter the energy levels of the system. The effect of the elastic deformations upon the paramagnetic ion can be described by a magnetoelastic tensor, the most important terms usually all being contained in a tensor of the fourth rank. Again the point-group symmetry of the site determines the form of the tensor, and the local tensors for magnetically inequivalent sites are related by the symmetry operations of the crystal space group. The magnetoelastic tensor of paramagnetic ions is of some importance for paramagnetic acoustic studies and in paramagnetic relaxation, and has been determined from the strain dependence of EPR spectra for several ions, usually for sites of high symmetry where the number of independent constants is small.[1–3]

We report in this paper the determination of the magnetoelastic tensors of Gd^{3+}, Yb^{3+}, and Er^{3+} in the diamagnetic gallium or aluminum garnets. The symmetry of the rare-earth site in the garnet structure is low (orthorhombic) so the magnetoelastic tensor has a large number (12) of independent constants. To reduce the number of independent constants we have examined the general magnetoelastic tensor for "hidden" symmetries which imply relationships between some of the parameters not given by the site-point symmetry alone. For instance, conservation of the trace of the crystalline electric field tensor under strain implies constraints connecting certain elements of the magnetoelastic tensor.

We were motivated to pursue the fairly involved task of establishing these single-ion magnetoelastic tensors

* Work supported in part by the Advanced Research Projects Agency through the Center for Materials Research at Stanford University and in part by the National Science Foundation through NSF Grant No. GK-202.
† Permanent address: The Clarendon Laboratory, Oxford University, Oxford, England.

[1] E. R. Feher, Phys. Rev. **136**, A145 (1964).
[2] E. B. Tucker, Phys. Rev. **143**, 264 (1966).
[3] G. D. Watkins and E. R. Feher, Bull. Am. Phys. Soc. **7**, 29 (1962).

primarily because of the connection they bear to the macroscopic magnetoelastic tensor of the ordered rare-earth iron garnets. The magnetoelastic properties of the rare-earth garnets have become of some technological and scientific interest recently, especially with relation to magnetoacoustics. The magnetoelastic constants (e.g., magnetostriction constants) of the rare-earth garnets are known to depend mainly on the rare-earth ion involved,[4] and it is our primary purpose to explain the observed magnetoelastic parameters in the rare-earth garnets, starting from the single-ion, rare-earth magnetoelastic tensor determined from EPR data on diamagnetic garnet crystals subject to stress. The earlier sections of this paper therefore deal with the properties and determination of the single-ion (local or microscopic) magnetoelastic tensors for the rare-earth ions, and the later sections deal with the utilization of these single-ion microscopic parameters to predict the macroscopic magnetoelastic properties of the ordered magnetic garnets.

2. THE SINGLE-ION MAGNETOELASTIC TENSOR

The single-ion magnetoelastic tensor describes that portion of the magnetic energy of an ion which depends on the state of strain of the host crystal. If one expands the magnetic energy E_M as a Taylor series in the lattice strains about the equilibrium configuration,

$$E_M=(E_M)_0+\sum_k\sum_l(\partial E_M/\partial\epsilon_{kl})_0\epsilon_{kl}+\cdots, \quad (2.1)$$

the linear magnetoelastic energy is given by

$$E_{ME}=\sum_k\sum_l(\partial E_M/\partial\epsilon_{kl})_0\epsilon_{kl}. \quad (2.2)$$

This magnetoelastic energy is generally described by a fourth-rank tensor $\mathbf{B}$, of the form

$$E_{ME}=\sum_i\sum_j\sum_k\sum_l B_{ijkl}\alpha_i\alpha_j\epsilon_{kl}, \quad (2.3)$$

where α_i and α_j are direction cosines of the magnetic moment and the ϵ_{kl} are, of course, strains in Love's notation. For an ion in a given site symmetry, the form of these tensors can be obtained by requiring that the tensors be invariant under the operations of the group appropriate to the site symmetry.[5] It occasionally happens that such a tensor has additional symmetry derived from some characteristic of the phenomenon being described. For instance, the familiar elastic (stress-strain) tensor, also a fourth-rank tensor, is symmetric across the diagonal because the elastic energy it represents is invariant under the interchange of stress and strain coordinates. It has been implied[6] that the magnetoelastic tensor is similarly symmetric across the diagonal. We wish to argue here that such is not generally the case on theoretical grounds and shall subsequently find that such is not the case experimentally for the rare-earth ions in the garnets.

Let us examine what physical mechanisms underlie the single-ion magnetoelastic tensor. We may do so by writing the magnetic portion of the single-ion Hamiltonian and examining its strain dependence. For the lowest-lying manifold of states (in which we are generally interested) we may write a spin Hamiltonian

$$\mathcal{H}_M=\beta\mathbf{H}^\circ\cdot\mathbf{g}\cdot\mathbf{S}+\mathbf{S}\cdot\mathbf{D}\cdot\mathbf{S}+\text{terms in } S^4,\ S^6. \quad (2.4)$$

The magnetoelastic tensor is given by the strain dependence of $\mathcal{H}_M$, and is

$$\mathcal{H}_{ME}=\beta\sum_{ijkl}\left(\frac{\partial g_{ij}}{\partial\epsilon_{kl}}\right)_0 H_i^\circ S_j\epsilon_{kl}+\sum_{ijkl}\left(\frac{\partial D_{ij}}{\partial\epsilon_{kl}}\right)_0 S_iS_j\epsilon_{kl}$$

$$+(\text{terms higher order in the spin coordinates}). \quad (2.5)$$

The terms in the magnetoelastic energy derived from the spin-Hamiltonian terms of order S^4, S^6, etc., are not of interest to us at present because (a) they do not contribute to the fourth-rank magnetoelastic tensor (but to a higher-rank tensor) and (b) because their contribution to the total magnetoelastic energy is (fortunately) quite small.

For sites of high symmetry (e.g., cubic) it may be that $(\mathbf{D})_0=0$, i.e., that the equilibrium value of $\mathbf{D}$ is zero, but strains which reduce this symmetry introduce an energy quadratic in the spin coordinates, so that $(\partial D_{ij}/\partial\epsilon_{kl})_0\neq0$ and the second term of Eq. (2.5) remains important in the magnetoelastic behavior of the ion. Such a situation occurs for the transition-metal ions in MgO.[7]

We note that the important atomic parameters entering the magnetoelastic energy are $(\partial g_{ij}/\partial\epsilon_{kl})_0=F_{ijkl}$, the strain dependence of the $\mathbf{g}$ tensor, and $(\partial D_{ij}/\partial\epsilon_{kl})_0=G_{ijkl}$, the strain dependence of the crystal-field components. We may therefore examine these derivatives for "hidden" symmetry, and in particular we shall examine the F_{ijkl} and G_{ijkl} tensors for symmetry across the diagonal. For instance, we wish to see if

$$F_{ijkl}=(\partial g_{ij}/\partial\epsilon_{kl})_0\stackrel{?}{=}(\partial g_{kl}/\partial\epsilon_{ij})_0=F_{klij}. \quad (2.6)$$

We make this examination through the vehicle of a point-ion calculation. Though such a calculation may not lead to quantitatively reliable predictions, it is certain that parameters predicted to be unequal on such a simplified model are not likely to become equal on a more complicated model, though the converse might happen. We consider in particular an octahedrally coordinated paramagnetic ion (Fig. 1) with neighbors of equal charge Ze situated at $x=\pm a$,

[4] A. E. Clark, B. F. DeSavage, N. Tsuya, and S. Kawakami, J. Appl. Phys. **37**, 1434 (1966).
[5] W. I. Dobrov, Phys. Rev. **134**, A734 (1964).
[6] R. B. Hemphill, P. L. Donoho, and E. D. McDonald, Phys. Rev. **146**, 327 (1966).
[7] T. G. Phillips and R. L. White, Phys. Rev. **153**, 616 (1967).

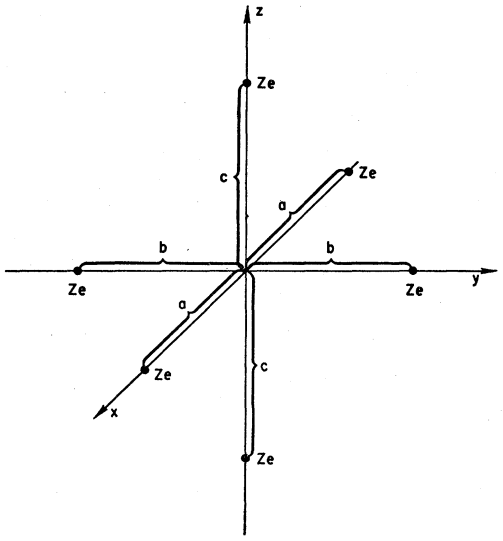

FIG. 1. Ion coordination octahedron for point-ion crystal-field calculation.

$y=\pm b$, and $z=\pm c$. The crystal field at the origin may be calculated quite straightforwardly, and that portion of the crystal field quadratic in the spin components,

$$V_2=D_{11}S_x^2+D_{22}S_y^2+D_{33}S_z^2, \tag{2.7}$$

has the crystal-field coefficients

$$D_{11}=Ze^2\alpha\langle r^2\rangle\left[\frac{3}{2}\left(\frac{1}{a^3}-\frac{1}{b^3}\right)-\left(\frac{1}{c^3}-\frac{1}{2b^3}-\frac{1}{2a^3}\right)\right],$$

$$D_{22}=Ze^2\alpha\langle r^2\rangle\left[\frac{3}{2}\left(\frac{1}{b^3}-\frac{1}{a^3}\right)-\left(\frac{1}{c^3}-\frac{1}{2b^3}-\frac{1}{2a^3}\right)\right],$$

$$D_{33}=Ze^2\alpha\langle r^2\rangle\left[2\left(\frac{1}{c^3}-\frac{1}{2b^3}-\frac{1}{2a^3}\right)\right], \tag{2.8}$$

where α and $\langle r^2\rangle$ have the meanings introduced by Elliot and Stevens.[8] We may compute some G_{ijkl} by taking the derivatives of the D_{ii} with respect to a, b, and c (ϵ_{xx}, ϵ_{yy}, ϵ_{zz}). We also at this point introduce the Voigt notation ($\epsilon_{xx}=\epsilon_1$, $\epsilon_{yy}=\epsilon_2$, $\epsilon_{zz}=\epsilon_3$, $\epsilon_{yz}=\epsilon_4$, etc.) to simplify our subscripting. In this notation we find, for instance,

$$G_{12}=(\partial D_{11}/\partial\epsilon_{yy})_0=(\partial D_{11}/\partial b)_0=+3K/b_0^4,$$
$$G_{21}=(\partial D_{22}/\partial\epsilon_{xx})_0=(\partial D_{22}/\partial a)_0=+3K/a_0^4, \tag{2.9}$$

where $K=Ze^2\alpha\langle r^2\rangle$. Clearly $G_{12}\neq G_{21}$, except in the tetragonal limit, in which case symmetry would have required their equality. Indeed, if one examines all the conjugate pairs, one finds that the G_{ij} tensor is symmetric only in the limit of cubic symmetry. The apparent symmetry across the diagonal of the magnetoelastic tensor of Cr^{3+} in Al_2O_3 observed by Hemphill *et al.*[6] is probably related to the near cubicity of the Cr^{3+} octahedral environment; such symmetry is neither expected nor found for the badly distorted rare-earth site in the garnets.

We may also on the point-ion model deduce something about the symmetry of the F_{ijkl} tensor, important when the lowest-lying state is a Kramers's doublet and changes in the **g** tensor are responsible for the magnetoelastic energy. The simplest case useful for such a calculation occurs for an ion of $S=\frac{3}{2}$ situated in the crystal field of Eq. (2.8). The crystal field produces an energy-level scheme consisting of two Kramers's doublets, one of which has the g values

$$g_{xx}=2g(\cos^2\chi-\sqrt{3}\,\sin\chi\,\cos\chi),$$
$$g_{yy}=2g(\cos^2\chi+\sqrt{3}\,\sin\chi\,\cos\chi),$$
$$g_{zz}=2g\,\sin 2\chi, \tag{2.10}$$

where

$$\tan 2\chi=(D_{11}-D_{22})/\sqrt{3}D_{33}. \tag{2.11}$$

From Eqs. (2.10) and (2.11) it is quite straightforward though algebraically involved to calculate the $F_{ijkl}=\partial g_{ij}/\partial\epsilon_{kl}$. The results are generally somewhat complicated expressions, but we can inspect them in some simple limits. For instance, in the tetragonal limit, $a_0=b_0$, $\tan 2\chi=0$, we find that

$$F_{12}=(\partial g_{xx}/\partial a)_0=F_{21}=(\partial g_{yy}/\partial a)_0 \tag{2.12}$$

as would be expected from the tetragonal symmetry, but that

$$F_{13}=(\partial g_{xx}/\partial c)_0=-2F_{31}=-2(\partial g_{zz}/\partial a)_0. \tag{2.13}$$

Not only are the conjugate elements unequal, but they may be of opposite sign. As we shall see, conjugate pairs of opposite sign appear, in fact, to be the rule rather than the exception for the rare-earth Kramers's ions in the garnets.

The above arguments lead us to conclude that the magnetoelastic tensor is not in principle symmetric across its diagonal.

Examination of the microscopic origins of the magnetoelastic tensor does lead us, however, to some useful conclusions regarding the reduction of the number of independent constants arising from the invariance under strain of the trace of **D** or of **g**. We first examine the tensor G_{ijkl} derived from the crystal-field tensor **D**, which is known to be traceless.[5,9] If the difference between the tensor **D** before and after the introduction of a strain ϵ is the tensor **d**, then the trace of **d** must also be zero. Now

$$d_{ij}=\sum_{kl}G_{ijkl}\epsilon_{kl} \tag{2.14}$$

from the definition of G_{ijkl}, and the tracelessness of **d**

[8] K. W. H. Stevens, Proc. Phys. Soc. (London) **A65**, 209 (1952); R. J. Elliot and K. W. H. Stevens, *ibid.* **A218**, 553 (1953).

[9] R. G. Shulman, B. S. Wyluda, and P. W. Anderson, Phys. Rev. **107**, 953 (1951).

may be written

$$\sum_i d_{ii}=\sum_{ikl} G_{iikl}\epsilon_{kl}=0 \qquad (2.15)$$

for all ϵ, from which we conclude that

$$\sum_i G_{iikl}=0 \quad \text{for all } kl. \qquad (2.16)$$

For our orthorhombic site symmetry this constraint will reduce the number of independent constants from 12 to 9.

If the trace of the **g** tensor is invariant under strain the same logic will apply to the **F** tensor. In general, unfortunately, the trace of the **g** tensor is not invariant under strain. We shall argue here, however, that there commonly occur circumstances under which the variation in the trace of **g** contains no terms linear in the strains, a condition sufficient for our earlier arguments to apply and the number of independent constants in the magnetoelastic to be reduced. Consider first an ion in a site of cubic symmetry. The **g** tensor will be isotropic, with value g_c and trace equal to $3g_c$. Now suppose the site is distorted to some lower symmetry. We may expand the principal g values in the lower-symmetry fields produced by the distortion

$$g_1=g_c+c_1^{120}V_2^0+c_1^{122}V_2^2+\cdots+c_1^{220}(V_2^0)^2+\cdots,$$
$$g_2=g_c+c_2^{120}V_2^0+c_2^{122}V_2^2+\cdots+c_2^{220}(V_2^0)^2+\cdots,$$
$$g_3=g_c+c_3^{120}V_2^0+c_3^{122}V_2^2+\cdots+c_3^{220}(V_2^0)^2+\cdots. \qquad (2.17)$$

We therefore have

$$\text{trace } \mathbf{g}=3g_c+(\sum_i c_i^{1nm})V_n^m+(\sum_i c_i^{2nm})(V_n^m)^2+\cdots. \qquad (2.18)$$

Finally, let us strain the crystal, changing each crystal-field component to $(V_n^m)_0+(\partial V_n^m/\partial\epsilon_{kl})_0\epsilon_{kl}$. We will then have, for each strain component ϵ_{kl},

$$\delta(\text{trace } \mathbf{g})=(\sum_i c_i^{1nm})(\partial V_n^m/\partial\epsilon_{kl})_0\epsilon_{kl}+(\sum_i c_i^{2nm})2V_n^m(\partial V_n^m/\partial\epsilon_{kl})_0\epsilon_{kl}+(\text{higher-order terms}). \qquad (2.19)$$

We now point out that if it was observed for the ion involved that the trace of **g** for the distorted site was substantially equal to $3g_c$, it is implied that the expansion coefficients $(\sum_i c_i^{1nm})$ are all substantially zero, and that the trace of **g** will be invariant under the applied strain ϵ. The argument may be qualitatively rephrased that if the equilibrium distortions have not changed the trace of **g** from the isotropic value, then small additional strains will not change the trace either. We shall subsequently inspect specific ions in the garnet, and if trace $\mathbf{g}=3g_c$, we will assume

$$\sum_i(\partial g_{ii}/\partial\epsilon_{kl})_0\epsilon_{kl}=\sum_i F_{iikl}\epsilon_{kl}=0, \qquad (2.20)$$

again reducing (for the orthorhombic case) the 12 independent constants of the magnetoelastic tensor to nine.

Finally, in this section, we wish to make a point which is important but nevertheless often ignored. The local tensors found from stress work are defined with respect to unit-cell strains and not the local environment strains. Therefore we cannot make a quantitative comparison with any crystal-field theory unless we know the tensor relating the unit-cell strains to the local environment strains. To our present knowledge, no determination of such a tensor has yet been attempted.

3. THE DETERMINATION OF THE MAGNETOELASTIC TENSOR FROM EPR PRESSURE EXPERIMENTS

We have seen in the preceding section that the single-ion magnetoelastic tensor is determined by the strain dependence of the **g** tensor and the crystal-field **D** tensor of the spin Hamiltonian of the ion. Since the **g** tensor and **D** tensor may be determined from electron-paramagnetic-resonance experiments we may be sure that the strain dependence of these parameters may be obtained from the strain dependence of EPR spectra. There are on the order of ten independent constants in the magnetoelastic tensor to be determined, so it is desirable to develop some systematic procedure relating the desired parameters to the experimental variables, which are the magnitude and direction of an axial pressure **P** and the magnitude and direction of a magnetic field **H°**.

As we can see from Eq. (2.5), there are two kinds of terms in the magnetoelastic tensor, those arising from $\partial g_{ij}/\partial\epsilon_{kl}$ and those arising from $\partial D_{ij}/\partial\epsilon_{kl}$. Usually only one or the other class of terms is important. If the ion is an S-state ion ($L=0$), the strain dependence of the **g** tensor is vanishingly small and the $\partial D_{ij}/\partial\epsilon_{kl}$ terms dominate. If the ion is not an S-state ion and the ground state displays spin or orbital degeneracy, the $\partial g_{ij}/\partial\epsilon_{kl}$ term is generally (but not necessarily) more important. For the odd-electron rare-earth ions, a single Kramers's doublet usually lies lowest in energy; for a Kramers's doublet with effective spin $\frac{1}{2}$ we have $\mathbf{D}\equiv 0$ and the $\partial g_{ij}/\partial\epsilon_{kl}$ effect is clearly dominant.

Let us consider then two common cases; the S-state ion and the Kramers's doublet ion.

A. S-State Ions

The spin Hamiltonian of the S-state ion in the unstrained crystal will be

$$\mathcal{H}=g\beta H_z^0S_z+D_{11}S_{x'}^2+D_{22}S_{y'}^2+D_{33}S_{z'}^2+D_{12}(S_{x'}S_{y'}+S_{y'}S_{x'})+D_{23}(S_{y'}S_{z'}+S_{z'}S_{y'})+D_{31}(S_{z'}S_{x'}+S_{x'}S_{z'}), \qquad (3.1)$$

where g will be taken to be isotropic and strain-inde-

pendent. We will choose to quantize along the axis of the magnetic field, the z axis, since the dominant energy term will be the Zeeman term. On the other hand we want the magnetoelastic tensor in terms of the local site coordinates x', y', z'. The **D** tensor and **g** tensor will ordinarily be diagonal in this coordinate frame in the unstrained crystal, but no longer diagonal in the strained crystal. In anticipation of the strained case we treat **D** as nondiagonal in Eq. (3.1). The magnetic field H_z° has the direction cosines α_1, α_2, α_3 in the local (primed) coordinate frame.

If we conduct our experiments under circumstances such that the first term in Eq. (3.1) dominates, we may use first-order perturbation theory to treat the crystal-field terms and the problem is greatly simplified. The example appropriate to this investigation is Gd^{3+} ($S=\frac{7}{2}$), and the energy levels will be

$$\begin{aligned}
E_{\pm 7/2}&=\pm\tfrac{7}{2}g\beta H^\circ+\tfrac{42}{4}\sum_{ij} D_{ij}\alpha_i\alpha_j,\\
E_{\pm 5/2}&=\pm\tfrac{5}{2}g\beta H^\circ+\tfrac{6}{4}\sum_{ij} D_{ij}\alpha_i\alpha_j,\\
E_{\pm 3/2}&=\pm\tfrac{3}{2}g\beta H^\circ+\tfrac{18}{4}\sum_{ij} D_{ij}\alpha_i\alpha_j,\\
E_{\pm 1/2}&=\pm\tfrac{1}{2}g\beta H^\circ-\tfrac{30}{4}\sum_{ij} D_{ij}\alpha_i\alpha_j. \qquad (3.2)
\end{aligned}$$

The difference in energy between states—the transition energies—are given by

$$E_{S_1}-E_{S_2}=g\beta H^\circ(S_1-S_2)+\tfrac{3}{2}(S_1^2-S_2^2)\sum_{ij} D_{ij}\alpha_i\alpha_j. \qquad (3.3)$$

If we impose now a stress on the crystal, strains are developed such that

$$\boldsymbol{\varepsilon}=\mathbf{S}\cdot\mathbf{P}, \qquad (3.4)$$

where **S** is the compliance tensor. The strains cause changes in the components of the **D** tensor

$$\delta D_{ij}=\sum_{kl} G_{ijkl}\epsilon_{kl}, \qquad (3.5)$$

so the change in $\sum_{ij} D_{ij}\alpha_i\alpha_j$ of the transition-energy expression of Eq. (3.3) is

$$\delta\sum_{ij} D_{ij}\alpha_i\alpha_j=\sum_{ijkl} G_{ijkl}\alpha_i\alpha_j\epsilon_{kl}. \qquad (3.6)$$

One can then apply a known stress **P**, obtaining a known $\boldsymbol{\varepsilon}$ (set of ϵ_{kl}), apply the magnetic field in a known direction (α_i, α_j) and observe the change in transition energy $\delta(E_{S_1}-E_{S_2})$. Inserting the known ϵ_{kl} and α_i into Eq. (3.6) then yields one equation in several unknowns, the G_{ijkl}. A second experiment with the pressure in a different direction, or the magnetic field in a different direction, or both, yields a second equation in the several unknowns. A number of independent experiments at least equal to the number of independent G_{ijkl} must be performed, and the resultant set of equations solved simultaneously to yield the several G_{ijkl}.

A further calculational difficulty is that the compliance tensor **S** is generally given in the unit-cell crystal axes rather than in the local x', y', z' axes. Clearly the strains and directions cosines of Eqs. (3.5) and (3.6) must be in the same coordinate frame, so either the **S** tensor or the **G** tensor must be transformed. We have elected to transform the **G** tensors to the crystal axes and work in that frame, since that is the frame with respect to which the applied fields and stresses are measured. The required transformations are discussed in the next section and in the Appendix.

If the Zeeman energy is not sufficiently greater than the crystal-field energies such that first-order perturbation theory can be applied, a much more complicated computational procedure must be followed. Such a case, Fe^{3+} in Al_2O_3, will be treated in a separate paper.

B. Non-S-State Ions

If the ground state of the ion is a Kramers's doublet the procedure is somewhat simpler. In view of the effective spin of $\frac{1}{2}$ the crystal-field terms vanish identically, and the effective spin Hamiltonian is simply

$$\mathcal{H}=\beta\mathbf{H}^\circ\cdot\mathbf{g}\cdot\mathbf{S}'. \qquad (3.7)$$

The changes in **g** due to strain will be given by

$$\delta g_{ij}=\sum_{kl} F_{ijkl}\epsilon_{kl} \qquad (3.8)$$

and the change in transition energy by

$$\delta E=\tfrac{1}{2}\beta H^\circ\sum_{ijkl} F_{ijkl}\alpha_i\alpha_j\epsilon_{kl}. \qquad (3.9)$$

Again one applies strains and the magnetic field in several combinations until enough independent equations are obtained to determine the several F_{ijkl}.

If the ground state has an effective spin greater than $\frac{1}{2}$ it may be difficult to separate changes in resonance field due to $\delta\mathbf{g}$ and $\delta\mathbf{D}$. The second-order effect in $\delta\mathbf{D}$ appears as an apparent $\delta\mathbf{g}$, and we may require a wide range of pressures to separate the linear from the quadratic effects, or operate using special transitions which are independent of one effect or the other. Such a case occurs for Fe^{2+} in MgO, for which the ground state has an effective spin of 1.[7]

4. SITE SYMMETRY AND INEQUIVALENT SITES IN THE GARNET STRUCTURE

Turning our attention to the specific system at hand, we now examine the site symmetry and site inequivalences which exist for rare-earth ions in the garnet structure.

The over-all symmetry of the garnet is cubic, O_h^{10}–$1a3d$, and the rare-earth (and yttrium) ions occupy the dodecahedral positions 24(c). The local site symmetry is orthorhombic and the eight oxygen near

neighbors are arranged at the corners of a fairly heavily distorted cube.[10] For one site the local axes lie along crystal ⟨001⟩, ⟨110⟩, and ⟨1$\bar{1}$0⟩ directions, and the others of the six inequivalent sites may be obtained from this site by the transformations described in the Appendix.

From Dobrov[5] we know the form of the magnetoelastic tensor for this particular (orthorhombic) site symmetry. Expressed in the local major axis system both the **G** and **F** tensors are of the same form, and are the same for all six inequivalent sites. In the Voigt notation

$$\mathbf{G}=\begin{bmatrix} G_{11} & G_{12} & G_{13} & 0 & 0 & 0 \\ G_{21} & G_{22} & G_{23} & 0 & 0 & 0 \\ G_{31} & G_{32} & G_{33} & 0 & 0 & 0 \\ 0 & 0 & 0 & G_{44} & 0 & 0 \\ 0 & 0 & 0 & 0 & G_{55} & 0 \\ 0 & 0 & 0 & 0 & 0 & G_{66} \end{bmatrix}. \tag{4.1}$$

There are 12 independent constants in this tensor; the trace invariance of **g** or **D** will reduce the number of independent constants to 9 [cf. Eqs. (2.16) or (2.20)].

The **G** tensor above is written in the local site axis coordinate frame; we need **G** in the crystal-axis coordinate frame since the stresses and strains are known in that coordinate frame. The fourth-rank tensor transformation is

$$G'_{ijkl}=\sum_{mnop} a_{im}a_{jn}a_{ko}a_{lp}G_{mnop}, \tag{4.2}$$

where the a_{im} are direction cosines between the primed and crystal-coordinate axes. For the site whose principal local axes are crystal ⟨001⟩, ⟨110⟩, and ⟨1$\bar{1}$0⟩ axes, the tensor **G** of Eq. (4.1) becomes, in the crystal-coordinate frame,

$$\mathbf{G}'=\begin{bmatrix} G'_{11} & G'_{12} & G'_{13} & 0 & 0 & G'_{16} \\ G'_{21} & G'_{22} & G'_{23} & 0 & 0 & G'_{26} \\ G'_{31} & G'_{32} & G'_{33} & 0 & 0 & G'_{36} \\ 0 & 0 & 0 & G'_{44} & G'_{45} & 0 \\ 0 & 0 & 0 & G'_{54} & G'_{55} & 0 \\ G'_{61} & G'_{62} & G'_{63} & 0 & 0 & G'_{66} \end{bmatrix}. \tag{4.3}$$

The relationships between the G_{ij} and the G'_{ij} are given in the Appendix. Though **G′** is no longer in the "block" form as was **G**, the number of independent elements has not increased.

[10] S. Geller and M. A. Gilleo, J. Phys. Chem. Solids **3**, 30 (1957).

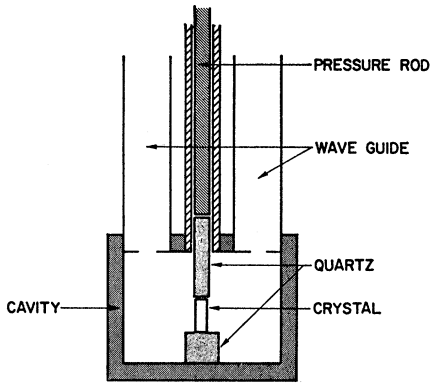

FIG. 2. Microwave cavity showing mechanism for applying uniaxial pressure to crystal.

We may proceed to write the **G′** tensors for the remaining five inequivalent sites in the crystal-coordinate frame. In the crystal axis system, the **G′** tensors for the six inequivalent sites all look different from one another. In the Appendix we obtain the tensors **G′** for all the six inequivalent sites. Though the existence of the six inequivalent sites is quite a complication theoretically, it nonetheless has its compensations. If one observes transitions from all six sites, the application of any one direction of pressure and one direction of magnetic field constitutes six experiments for the determination of the G_{ij}, and drastically reduces the number of experimental configurations necessary to determine the 12 (or nine after trace considerations) independent G_{ij}.

5. EXPERIMENTAL PROCEDURES

Electron paramagnetic experiments were carried out using a conventional microwave spectrometer working at 26 *k*Mc/sec. A direct detection system was employed, and the field-modulation frequency was 400 cps. The microwave cavity was used in the TE_{011} mode in transmission, and the klystron frequency was locked to the cavity frequency both to improve the signal-to-noise ratio and to eliminate any dispersion which might interfere with the pure absorption line shape. A helium Dewar was fitted and the system could be operated at 77°K or 4.2→1.5°K.

The specimen crystal was cut with end faces flat and parallel to optical tolerances and mounted in the center of the cavity (see Fig. 2) on a quartz block. The microwave cavity thus also acts as the pressure cavity. Pressure was applied by means of a quartz plunger, itself driven by a steel rod and a system of weights and levers. The quartz block and plunger were also optically cut and polished, but in spite of this it was found necessary to employ buffer pads between the pressure surfaces in order to achieve a homogeneous pressure within the specimen. It appears that these pads can be made of almost any material which is initially relatively soft, but sets hard under pressure or

low temperatures. In our case, thin plastic sheet was found quite suitable and we were able to generate pressure of the order of 10^4 kg/cm^2 without breaking the crystals. Since the microwave cavity was also the pressure cavity, its resonance frequency was a mild function of the applied pressure. This pressure dependence of the frequency was measured and corrected out in processing the data.

The experimental configuration described above has the advantages of simplicity of construction, ease of pressure measurement, and the facility to work on crystals of almost any size. In point of fact the most convenient crystal volume was about 10 mm^3. There is, however, a major possible disadvantage in that one cannot arrange for the dc magnetic field of a normal iron-cored EPR magnet to be parallel to the pressure axis This could prevent the independent determination of all the elements of **G** and **F**, but it is found that the assumption of constant trace for **D** and **g** as discussed in Sec. 2 alleviates this difficulty and one can obtain all the elements even with the magnetic field confined to a plane normal to the pressure axis.

6. SINGLE-ION MAGNETOELASTIC TENSOR FOR Gd^{3+} IN THE GARNETS

Trivalent gadolinium has a ground state which is a spectroscopic S state with electronic spin $S=\frac{7}{2}$. The theory of Sec. 3A for the extraction of the **G** tensor from the EPR data is therefore appropriate The EPR spectrum of Gd^{3+} in yttrium gallium garnet (YGaG) in the unstrained crystal has been studied by Rimai and Mars[11] and by Calhoun and Freiser,[12] and we have leaned upon their work in identifying the transitions observed. In particular it is necessary to know the sign of the components of **D** to obtain correctly the signs of δ**D**.

Since **D** is traceless we know that the 12 independent constants of **G** are reduced to nine for the Gd^{3+} case, and our problem experimentally is to apply pressures and magnetic fields in such combinations as to obtain the required nine independent equations; preferably equations as simple as possible (involving the fewest ϵ_{kl}, for instance). There are several experimental difficulties in this procedure, mostly derived from the fact that the six inequivalent sites each yield seven allowed transitions, giving an overlapping 42-line spectrum which makes identification and measurement of specific transition-energy changes difficult. If the magnetic field is applied in certain major crystallographic directions, the spectrum collapses considerably but site identification is lost. One exceptional and useful case is that with H° along a crystal $\langle 110\rangle$. In this instance, the six spectra are distributed such that the two which are derived from ions having a local principal axis along $\langle 110\rangle$ are spread out in field and are resolved from one another while the remaining four spectra are bunched near the center of the patterns and are not separately identifiable nor useful. The experimental setup requires the stress to be applied perpendicular to H°; therefore, several independent equations were obtained with H° along a $\langle 110\rangle$ and uniaxial strains applied in major directions ($\langle 001\rangle$ and $\langle 1\bar{1}0\rangle$) perpendicular to $\langle 110\rangle$. It is not possible to obtain the required number of independent equations using this configuration alone, since certain linear combinations of the G_{ijkl} and ϵ_{kl} recur for all combinations of this class. To obtain the remaining independent equations it proved necessary to apply both the pressure and H° in some general direction not contained in a $\langle 110\rangle$ plane. Site identification was achieved for the general orientation of H° by plotting the whole 42-line spectrum for the plane containing the general direction and a high-symmetry direction of known site identification, preferably the $\langle 110\rangle$.

Proceeding in the above manner sufficient independent equations were obtained to allow determination of the nine independent constants of **G**. Expressed in the local site axis system (see Appendix) the magnetoelastic **G** tensor for Gd^{3+} in YGaG is

$$\mathbf{G}= \begin{array}{c} \\ \alpha_x^2 \\ \alpha_y^2 \\ \alpha_z^2 \\ \alpha_y\alpha_z \\ \alpha_z\alpha_x \\ \alpha_x\alpha_y \end{array} \begin{array}{c} \begin{array}{cccccc} \epsilon_{xx} & \epsilon_{yy} & \epsilon_{zz} & \epsilon_{yz} & \epsilon_{zx} & \epsilon_{xy} \end{array} \\ \begin{bmatrix} 1.1 & -1.3 & 0.1 & 0 & 0 & 0 \\ -1.0 & 1.5 & -0.8 & 0 & 0 & 0 \\ 0.0 & -0.2 & 0.7 & 0 & 0 & 0 \\ 0 & 0 & 0 & 2.5 & 0 & 0 \\ 0 & 0 & 0 & 0 & 3.2 & 0 \\ 0 & 0 & 0 & 0 & 0 & 0.1 \end{bmatrix} \end{array} \times \mathrm{cm}^{-1}/(\text{unit strain}). \quad (6.1)$$

As we have made a simultaneous solution of nine linear equations the errors are rather hard to evaluate, but are estimated to be approximately $\pm 20\%$. Values of the elastic constants used to determine the elements of **G** are those of Clark and Strakna.[13]

We may comment on the symmetry of **G** in view of the discussion of Sec. 2. The tensor is nonsymmetric as presented here, but only in the case of G_{23} and G_{32} is the nonsymmetry clearly defined above the errors. Within experimental error it appears that conjugate elements have the same sign, as predicted by the point-ion calculation. It is also interesting to note that the diagonal elements are all uniformly of the opposite sign from the off-diagonal elements also as predicted by the single-ion model as may be verified by noting

[11] L. Rimai and G. A. deMars, J. Appl. Phys. **33,** 1254 (1962).
[12] B. A. Calhoun and M. J. Freiser, J. Appl. Phys. **34,** 1140 (1963).
[13] A. E. Clark and R. E. Strakna, J. Appl. Phys. **32,** 1172 (1961).

that $(\partial D_{11}/\partial a)_0 = -6K/a_0^4$, $(\partial D_{22}/\partial b)_0 = -6K/b_0^4$, etc., whereas all off-diagonal elements were of the form $(\partial D_{11}/\partial b)_0 = +3K/b_0^4$, $(\partial D_{11}/\partial c)_0 = +3K/c_0^4$, etc. (The sign of G_{13} is not determined within the experimental error.)

7. SINGLE-ION MAGNETOSTRICTION TENSOR FOR Yb^{3+} AND Er^{3+} IN THE GARNETS

Both Yb^{3+} and Er^{3+} have Kramers's doublets with effective spin of $\frac{1}{2}$ as their ground states in a garnet host. The theory of Sec. 3B therefore applies for the determination of their magnetoelastic tensor **F**. The spectra for both Yb^{3+} and Er^{3+} are considerably simpler than for Gd^{3+} since there is only one absorption/site (not counting hyperfine components) yielding a generally resolved six-line spectrum. The EPR spectra of both Yb^{3+} and Er^{3+} have been examined by Hall *et al.*,[14] and their work was used to help identify and locate the desired transitions.

We next examine whether or not we may assume invariance of the trace of **g** and reduce our 12 independent constants to nine. For Yb^{3+} in YGaG, the trace of **g** is $3.87+3.78+2.47=10.12$. The cubic Γ_7 doublet from which the state derives has an isotropic $g_c=3.42$, hence $3g_c=10.26$. Clearly the trace of g has not varied perceptibly and we may with confidence assume the invariance of trace **g**. For Er^{3+} in YAlG the situation is somewhat less clear. Here trace $\mathbf{g}=7.75+3.71+7.35=18.81$, while the cubic Γ_7 doublet from which the state is probably derived has $g_c=5.66$ and $3g_c=16.98$. We nonetheless will assume the invariance of trace **g** for this case also and examine later for the consequences of this somewhat marginal assumption.

For Yb^{3+} we have overdetermined the **F** tensor in order to verify the trace invariance assumption above and in order to provide a check on the transformation algebra, site identification, and symmetry assumptions of the general theory. By overdetermining the **F** tensor, we mean making more than nine independent experiments and verifying that different sets of nine independent equations lead to the same set of nine elements for **F**. The **F** tensor we obtain for Yb^{+3} is

$$\mathbf{F}=\begin{bmatrix} 113 & 85 & 42 & 0 & 0 & 0 \\ -81 & -153 & -55 & 0 & 0 & 0 \\ -32 & 68 & 13 & 0 & 0 & 0 \\ 0 & 0 & 0 & 6 & 0 & 0 \\ 0 & 0 & 0 & 0 & 37 & 0 \\ 0 & 0 & 0 & 0 & 0 & 47 \end{bmatrix} \text{ per unit strain,} \tag{7.1}$$

[14] M. Ball, G. Garton, M. J. M. Leask, D. Ryan, and W. P. Wolf, J. Appl. Phys. **32**, 2675 (1961).

where again the tensor is given in the local site axes. The error as determined from the overdetermination scatter is approximately ± 6 for all elements. This fairly large error arises primarily from the uncertainties associated with the simultaneous determination of nine independent parameters. If the tensor **F** were of higher symmetry and had fewer independent elements, these fewer elements could be more precisely obtained from EPR pressure spectra.

As anticipated by the point-ion calculation of Sec. 2, this tensor is not symmetric across the diagonal and has, in fact, conjugate elements regularly of opposite sign. If we assume symmetry for **F**, reducing the independent constants to 6, and proceed to overdetermine this tensor, we obtain totally inconsistent sets of elements from different sets of independent equations. It is therefore clear that the **F** tensor is not symmetric across its diagonal.

A similar procedure was followed to obtain an overdetermined **F** tensor for Er^{3+} in the aluminum garnet. The change from gallium garnet to aluminum garnet host was purely for reasons of sample availability. We find **F** for Er^{3+} in YalG, again in the local site axis frame, to be

$$\mathbf{F}=\begin{bmatrix} 120 & 225 & 21 & 0 & 0 & 0 \\ -10 & -285 & -23 & 0 & 0 & 0 \\ -110 & 58 & 2 & 0 & 0 & 0 \\ 0 & 0 & 0 & 30 & 0 & 0 \\ 0 & 0 & 0 & 0 & -126 & 0 \\ 0 & 0 & 0 & 0 & 0 & 25 \end{bmatrix} \text{ per unit strain.} \tag{7.2}$$

The errors in the Er^{3+} tensor are somewhat larger than for the Yb^{3+} tensor, again as determined from scatter in the overdetermination. The errors are approximately ± 25 for each element, so only five elements have been determined with any real certainty. The precision of the data is similar for Yb^{3+} and Er^{3+}, so we tentatively attribute the greater scatter in the Er^{3+} **F** tensor as due to the onset of breakdown of the trace invariance assumption.

8. THE PREDICTION OF MACROSCOPIC MAGNETOELASTIC CONSTANTS FROM THE SINGLE-ION F AND G TENSORS

We now consider the relationship between the microscopic magnetoelastic tensors derived above and the macroscopic magnetoelastic constants of the ordered magnetic rare-earth iron garnets.

The magnetoelastic energy of an ordered magnetic material may also be described through the agency of

a fourth-rank magnetoelastic tensor which we shall call B^0_{ijkl}:

$$E_{\mathrm{ME}}=\sum_{ijkl} B^0_{ijkl}\alpha_i\alpha_j\epsilon_{kl}, \tag{8.1}$$

where the α_i's are now direction cosines of the net magnetization. For the rare-earth iron garnets, of cubic O_h symmetry, there are only three independent constants in the B^0_{ijkl} tensor (B_{11}, B_{12}, and B_{44} in the Voigt notation). An implicit assumption of trace invariance is usually made, reducing the number of independent constants to two, so the magnetoelastic energy of the cubic ferromagnet (or ferrimagnet) is usually written[15]

$$E_{\mathrm{ME}}=B_1[(\alpha_1^2-\tfrac{1}{3})\epsilon_{xx}+(\alpha_2^2-\tfrac{1}{3})\epsilon_{yy}+(\alpha_3^2-\tfrac{1}{3})\epsilon_{zz}] +B_2[\alpha_1\alpha_2\epsilon_{xy}+\alpha_2\alpha_3\epsilon_{yz}+\alpha_3\alpha_1\epsilon_{zx}], \tag{8.2}$$

where $B_1(=B_{11}-B_{12})$ and $B_2(=2B_{44})$ are known as the first and second magnetoelastic constants. The magnetoelastic energy is often given alternatively in terms of the magnetostriction constants λ_{100} and λ_{111}, related to B_1 and B_2 by

$$\lambda_{100}=-\tfrac{2}{3}B_1/3(C_{11}-C_{12}) \qquad \lambda_{111}=-B_2/3C_{44}, \tag{8.3}$$

where the C_{ij} are the cubic elastic constants.

The constants B_1 and B_2 or λ_{100} and λ_{111} have been measured for a number of the rare-earth iron garnets,[4] are known to differ widely from one rare-earth garnet to the next, and to depend primarily on the rare-earth ion involved. We now ask if we can deduce the contribution of the rare-earth ions to the gross magnetoelastic energy of the ordered magnetic garnets from the single-ion magnetoelastic tensors derived as above from EPR under pressure.

The magnetoelastic energy due to the rare-earth ions will be derived from the strain dependence of the rare-earth ion magnetic energy in the ordered iron garnet. It is known from several kinds of evidence that a rare-earth ion in the iron garnets is exchange-coupled to certain of its iron neighbors with an interaction of moderate strength (exchange splittings on the order of 20–100 cm^{-1}) and coupled only very weakly to other rare-earth ions present. The iron ions are, in turn, strongly coupled amongst themselves with a Curie temperature of approximately 550°K, and are in a state of substantially complete alignment below 100°K, independent of the state of order of the rare-earth ions. To a very good approximation, then, the rare-earth ions may be thought of as existing quasiparamagnetically in an exchange field produced by the iron lattices. A molecular-field treatment of the rare-earth ion energy and magnetization should therefore be quite appropriate, and has in the past yielded excellent agreement when used to predict, for instance, the temperature dependence of rare-earth magnetization. We may describe therefore the energy of a typical rare-earth ion in the iron garnet by an expression quite analogous to Eq. (2.4)

$$\mathcal{H}_{\mathrm{M}}{}^{\sigma}=\beta\mathbf{H}_{\mathrm{eff}}{}^{\sigma}\cdot\mathbf{g}^{\sigma}\cdot\mathbf{S}+\mathbf{S}\cdot\mathbf{D}^{\sigma}\cdot\mathbf{S}, \tag{8.4}$$

where $\mathbf{H}^0$ has been replaced by the effective molecular field $\mathbf{H}_{\mathrm{eff}}$ (perhaps anisotropic) and the superscript σ has been introduced to index the six-inequivalent rare-earth sites. The magnetic energy per unit volume is clearly given by

$$\mathcal{H}_{\mathrm{M}}{}^{\circ}=\sum_{\sigma} N^{\sigma}\mathcal{H}_{\mathrm{M}}{}^{\sigma}, \tag{8.5}$$

where N^{σ} is the number of rare-earth sites of a particular kind per unit volume, and the magnetoelastic energy arising from this energy described by

$$\mathcal{H}^{\circ}{}_{\mathrm{ME}}=\sum_{ijkl}(\partial\mathcal{H}^{\circ}{}_{\mathrm{M}}(\alpha_i\alpha_j)/\partial\epsilon_{kl})_0\epsilon_{kl}. \tag{8.6}$$

Carrying out the derivative process above, we obtain for the magnetoelastic energy contribution of the rare-earth ions at low temperature, when all are in their lowest energy (maximum S_z) state,

$$E_{\mathrm{ME}}=\sum_{ijkl}\sum_{\sigma}[N^{\sigma}\beta H^{\sigma}{}_{\mathrm{eff}}(\partial g^{\sigma}{}_{ij}/\partial\epsilon_{kl})_0 S +N^{\sigma}C(\partial D^{\sigma}{}_{ij}/\partial\epsilon_{kl})_0 S^2]\alpha_i\alpha_j\epsilon_{kl}, \tag{8.7}$$

where

$$C=\langle g\mid \tfrac{1}{2}[3S_z^2-S(S+1)]\mid g\rangle/\langle g\mid S_z^2\mid g\rangle \tag{8.8}$$

is a quantum-mechanical correction for the difference between $[S(S+1)]^{1/2}$ and S, $\mid g\rangle$ being the ground state of the ion. In obtaining Eq. (8.7) from Eq. (8.4) we have ignored the strain dependence of $\mathbf{H}^{\sigma}{}_{\mathrm{eff}}$, which may be an important omission which we will discuss later. Comparing Eq. (8.7) with the general form [Eq. (8.1)] we observe that

$$B^0_{ijkl}=\sum_{\sigma} N^{\sigma}\beta H^{\sigma}{}_{\mathrm{eff}}SF^{\sigma}{}_{ijkl}+\sum_{\sigma} N^{\sigma}CS^2G^{\sigma}{}_{ijkl}. \tag{8.9}$$

We can therefore express the gross macroscopic magnetoelastic constants of the ordered rare-earth iron garnets at low temperatures if we know the microscopic single-ion rare-earth magnetoelastic tensor and the effective molecular field acting on the rare-earth ion.

We also note from Eq. (8.9) that the high-symmetry (cubic) B^0_{ijkl} tensor is obtained by a summation over sites of the low-symmetry (orthorhombic) B^{σ}_{ijkl}. This property of $\sum_{\sigma} B^{\sigma}_{ijkl}$ may be checked directly using the local magnetoelastic tensors given in the Appendix (expressed in unit-cell coordinates). This property also has experimental consequences in that any of the B^0_{ijkl} may be obtained from the EPR data by applying a specific strain ϵ_{kl} and a particular magnetic field (α_i, α_j) and summing transition displacements over the six inequivalent sites. This technique is particularly useful for predicting the magnetostriction constants λ_{100} and λ_{111}, since the first is yielded by applying pressure in a $\langle 100\rangle$ direction with some known field orientation and summing energy displacements over inequivalent sites

[15] C. Kittel, Rev. Mod. Phys. **21**, 541 (1949).

while the other may be obtained by applying pressure along a ⟨111⟩ direction and summing energy displacements over inequivalent sites.

9. PREDICTED AND OBSERVED MAGNETOSTRICTION CONSTANTS FOR GdIG, YbIG, AND ErIG

We now use the machinery and data generated above to predict the magnetostriction constants of gadolinium, ytterbium, and erbium iron garnets, and then compare these predictions with the experimental values of these parameters.

Gd^{3+} is an S-state ion, so the contribution of the gadolinium ions to the magnetoelastic constants or to the magnetostriction constants will be through the G^{σ}_{ijkl} terms of Eq. (8.9). Inserting the appropriate numerical values we obtain, for the Gd^{3+} contribution to the magnetostriction constants of GdIG,

$$\lambda_{100}(\mathrm{Gd}) = (4.2\pm2)\times10^{-6},$$
$$\lambda_{111}(\mathrm{Gd}) = (1.7\pm2)\times10^{-6}. \quad (9.1)$$

These values may be compared to the experimental values for the Gd^{3+} contribution, i.e., to $\lambda(\mathrm{GdIG}) - \lambda(\mathrm{YIG})$, at 4.2°K,[16]

$$\lambda_{100}(\mathrm{GdIG}) - \lambda_{100}(\mathrm{YIG}) = (8.2\pm2)\times10^{-6},$$
$$\lambda_{111}(\mathrm{GdIG}) - \lambda_{111}(\mathrm{YIG}) = (1.5\pm2)\times10^{-6}. \quad (9.2)$$

We note with satisfaction that the predicted magnetostriction contributions are of the correct sign and within a factor of 2 of the correct size. In view of the extrapolations and approximations involved, we regard this as quite satisfactory agreement. Only for Gd^{3+} of the ions considered is the rare-earth contribution to the magnetostriction small enough that the iron contribution must be subtracted from the observed total magnetostriction before comparison with the predictions is meaningful.

Both Yb^{3+} and Er^{3+} have Kramers's doublets lowest, so the major contribution to the magnetostriction comes through the F^{σ}_{ijkl} terms of Eq. (8.9). Note further that in the ordered magnetic garnets the rather small F^{σ}_{ijkl} are multiplied by a very large effective field producing a large total magnetoelastic energy. For Yb^{3+} in YbIG, using the effective molecular-field values obtained spectroscopically by Wickersheim[17] ($H_x=87\,200$, $H_y=153\,000$, $H_z=169\,000$ G) and the F^{σ}_{ijkl} of Sec. 7 we obtain predicted magnetostriction constants for YbIG of

$$\lambda_{100}(\mathrm{Yb}) = 82\times10^{-6}, \qquad \lambda_{111}(\mathrm{Yb}) = 34\times10^{-6}, \quad (9.3)$$

which we may compare with the measured values for YbIG (4.2°K)[18]:

$$\lambda_{100}(\mathrm{YbIG}) = 49\times10^{-6}, \qquad \lambda_{111}(\mathrm{YbIG}) = -27\times10^{-6}. \quad (9.4)$$

We note that, though the predicted magnetostriction constants are of approximately the correct magnitude, the predicted λ_{111} is of the wrong sign. Our input data for the Yb^{3+} case is probably the most precise of all our data, so the prediction is unambiguous. The failure of the model to produce the correct prediction is almost certainly due to the failure to include the strain dependence of the exchange field, $(\partial H^{\sigma}/\partial\epsilon_{kl})_0$, into our theory. It has been our hope that the topology of the exchange tensor **G**, defined by $\mathcal{H}_M = \mathbf{S}^1\cdot\mathbf{G}\cdot\mathbf{S}^2$, where $\mathbf{S}^1$ is an iron spin and $\mathbf{S}^2$ a rare-earth spin, would be sufficiently similar to that of the paramagnetic **g** tensor that the strain dependence of the exchange energy terms would have the same topology (and signs) as the strain dependence of the **g** tensor. Such an assumption yielded the correct magnitude and sign of the magnetostriction constants in the transition-metal monoxides FeO, CoO, and NiO.[7] Such seems not to be the case for Yb^{3+} in the garnet, so spectroscopic studies of the variation of the exchange splittings of Yb^{3+} in YbIG under uniaxial pressure are clearly in order to clarify the present dilemma.

For Er^{3+} we do not have detailed information on the exchange fields present, but inspection of the ErIG magnetization data and comparison with other rare-earth exchange parameters lead us to assume $H_{\mathrm{eff}}=190\,000$ G. Using this value and the F^{σ}_{ijkl} for Er^{3+} of Sec. 7, we obtain predicted magnetostriction constants for ErIG of

$$\lambda_{100}(\mathrm{Er}) = 216\times10^{-6}, \qquad \lambda_{111}(\mathrm{Er}) = -282\times10^{-6}. \quad (9.5)$$

The experimental values (extrapolated to low temperature rather than measured at low temperature in this case) are[4]

$$\lambda_{100}(\mathrm{ErIG}) = 420\times10^{-6}, \qquad \lambda_{111}(\mathrm{ErIG}) = -300\times10^{-6}. \quad (9.6)$$

For this case we predict in quite satisfactory manner the magnitude (large) and sign of the magnetoelastic constants. Again spectroscopic studies of the strain dependence of exchange splittings would be desirable to explain why the predictions are so accurate in this case but of wrong sign for Yb^{3+}.

10. CONCLUSIONS

We have determined the magnetoelastic tensors for Gd^{3+}, Yb^{3+}, and Er^{3+} substituted into the orthorhombic sites of the diamagnetic yttrium aluminum or yttrium gallium garnets. From these tensors it is clear that the orthorhombic tensor is not symmetric across the diagonal and that the **F** tensor is likely to contain conjugate elements of opposite sign whereas

[16] A. E. Clark and B. F. DeSavage (private communication).
[17] K. A. Wickersheim, Phys. Rev. **122**, 1376 (1961).
[18] P. J. Flanders, R. F. Pearson, and J. L. Page, Brit. J. Appl. Phys. **17**, 839 (1966).

the G tensor, though not symmetric, does not appear to contain conjugate elements of opposite sign. These symmetry conclusions are in agreement with arguments based on a simple single-ion calculation. The overdetermination technique indicates that the constant trace of the g tensor is a good approximation in the case of Yb^{3+} and a fair approximation for Er^{3+}.

A tensor transformation scheme has been developed for use in the multi-inequivalent ion case and has proved of use in analyzing the EPR pressure experiments and in the prediction of magnetostriction constants. It was noted, however, that the definition of these tensors has to be with respect to crystal unit cell strains and not the local strains on the ion environment. This circumstance unfortunately prevents any detailed comparison with a crystal theory of the origin of the tensors.

The connection between the microscopic single-ion magnetoelastic tensors and the macroscopic magnetoelastic tensor of the ordered rare-earth iron garnets was developed using a molecular-field single-ion Hamiltonian. This model allows an immediate division between the S-state ions and the non-S-state ions in terms of the mechanism by which they contribute to the total magnetoelastic energy. The S-state ions contribute only through the strain variation of the crystal-field D tensor, and generally produce small magnetoelastic energies. The non-S-state ions contribute through the strain dependence of g and generally lead to large magnetoelastic energies because the small variations in g are multiplied by a very large effective field producing large changes in the magnetic energy. The magnetostriction of non-S-state ions such as Yb^{3+} and Er^{3+} is one or two orders of magnitude greater than that of the S-state ion Gd^{3+}.

We have predicted magnetostriction constants for GdIG, YbIG and ErIG from EPR data and the above theory and compared these with experimental values. For GdIG and ErIG the agreement is quite satisfactory; for YbIG one of the magnetostriction constants is of the wrong sign. We feel that the probable reason for this discrepancy is that the strain dependence of the molecular field has been omitted from the theory.

ACKNOWLEDGMENTS

We wish to acknowledge the assistance of Richard L. Townsend, Jr. in the taking of the EPR spectra and in the performance of some of these calculations. We are indebted to Robert S. Feigelson of the Stanford Center for Materials Research and to Leon Soben of the Lockheed Palo Alto Research Laboratories for growing the garnet crystals used. We also wish to thank Dr. William Dobrov of the Lockheed Research Laboratories for stimulating discussions of these subjects. In particular, we are indebted to Dr. Dobrov for the arguments of Sec. 2 concerning the invariance of the trace of the g tensor under crystal distortions.[19]

[19] W. Dobrov, Phys. Letters **24A**, 501 (1967).

APPENDIX

The orthorhombic site magnetoelastic tensor G or F defined in an axis system x, y, z which corresponds to the major axis system of the local environment a, b, c is given by Dobrov[5] as

$$\mathsf{G}=\begin{bmatrix} G_{11} & G_{12} & G_{13} & 0 & 0 & 0 \\ G_{21} & G_{22} & G_{23} & 0 & 0 & 0 \\ G_{31} & G_{32} & G_{33} & 0 & 0 & 0 \\ 0 & 0 & 0 & G_{44} & 0 & 0 \\ 0 & 0 & 0 & 0 & G_{55} & 0 \\ 0 & 0 & 0 & 0 & 0 & G_{66} \end{bmatrix},$$

where all 12 elements are independent.

In the case of the rare-earth site in the garnet the major axes lie along the cube $\langle 001\rangle$, $\langle 110\rangle$, and $\langle 1\bar{1}0\rangle$ axes. If we wish to express G in the cube axes system we must transform G according to the fourth-rank tensor transformation

$$G'_{ijkl}=\sum_{mnop} a_{im}a_{in}a_{ko}a_{lp}G_{mnop}.$$

Thus tensor G′ referred to the cube axes x, y, z, is

$$\mathsf{G}'=\begin{bmatrix} G'_{11} & G'_{12} & G'_{13} & 0 & 0 & G'_{16} \\ G'_{21} & G'_{22} & G'_{23} & 0 & 0 & G'_{26} \\ G'_{31} & G'_{32} & G'_{33} & 0 & 0 & G'_{36} \\ 0 & 0 & 0 & G'_{44} & G'_{45} & 0 \\ 0 & 0 & 0 & G'_{54} & G'_{55} & 0 \\ G'_{61} & G'_{62} & G'_{63} & 0 & 0 & G'_{66} \end{bmatrix}.$$

The relations between G and G′ are

$$\begin{aligned}
&G'_{11}=G'_{22}=\tfrac{1}{4}(G_{11}+G_{12}+G_{21}+G_{22}+4G_{66}),\\
&G'_{12}=G'_{21}=\tfrac{1}{4}(G_{11}+G_{12}+G_{21}+G_{22}-4G_{66}),\\
&G'_{13}=G'_{23}=\tfrac{1}{2}(G_{13}+G_{23}),\\
&G'_{16}=G'_{26}=\tfrac{1}{4}(-G_{11}+G_{12}-G_{21}+G_{22}),\\
&G'_{31}=G'_{32}=\tfrac{1}{2}(G_{31}+G_{32}),\\
&G'_{33}=G_{33},\\
&G'_{36}=\tfrac{1}{2}(-G_{31}+G_{32}),\\
&G'_{44}=G'_{55}=\tfrac{1}{2}(G_{44}+G_{55}),\\
&G'_{45}=G'_{54}=\tfrac{1}{2}(G'_{44}-G'_{55}),\\
&G'_{61}=G'_{62}=\tfrac{1}{4}(-G_{11}-G_{12}+G_{21}+G_{22}),\\
&G'_{63}=\tfrac{1}{2}(-G_{13}+G_{23}),\\
&G'_{66}=\tfrac{1}{4}(G_{11}+G_{22}-G_{12}-G_{21}).
\end{aligned}$$

(Note well that there are 12 independent elements as before.)

If we take the above tensor G' to relate to site 1 [Fig. 3(a)], we have the following set of tensors for the six inequivalent sites for the garnet structure: Neglecting the prime,

tensor site 1 [Fig. 3(a)]:

$$\mathsf{G}^1=\begin{bmatrix} G_{11} & G_{12} & G_{13} & 0 & 0 & G_{16} \\ G_{12} & G_{11} & G_{13} & 0 & 0 & G_{16} \\ G_{31} & G_{31} & G_{33} & 0 & 0 & G_{36} \\ 0 & 0 & 0 & G_{44} & G_{45} & 0 \\ 0 & 0 & 0 & G_{45} & G_{44} & 0 \\ G_{61} & G_{61} & G_{63} & 0 & 0 & G_{66} \end{bmatrix},$$

tensor site 2 [Fig. 3(b)]:

$$\mathsf{G}^2=\begin{bmatrix} G_{11} & G_{12} & G_{13} & 0 & 0 & -G_{16} \\ G_{12} & G_{11} & G_{13} & 0 & 0 & -G_{16} \\ G_{31} & G_{31} & G_{33} & 0 & 0 & -G_{36} \\ 0 & 0 & 0 & G_{44} & -G_{45} & \\ 0 & 0 & 0 & -G_{45} & G_{44} & \\ -G_{61} & -G_{61} & -G_{63} & 0 & 0 & G_{66} \end{bmatrix},$$

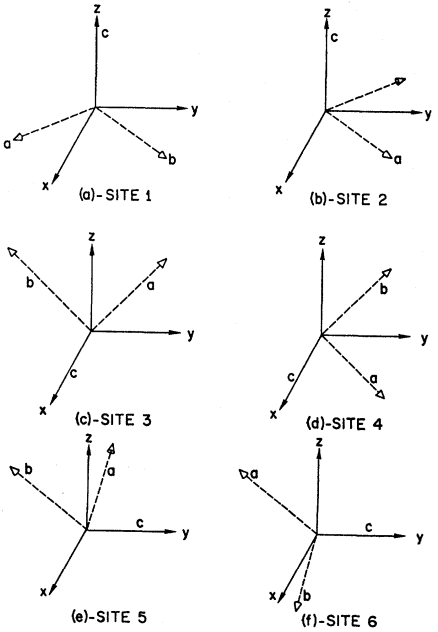

FIG. 3. Local coordinate frames for the various rare-earth sites relative to the crystal unit-cell axes.

tensor site 3 [Fig. 3(c)]:

$$\mathsf{G}_3=\begin{bmatrix} G_{33} & G_{31} & G_{31} & G_{36} & 0 & 0 \\ G_{13} & G_{11} & G_{12} & G_{16} & 0 & 0 \\ G_{13} & G_{12} & G_{11} & G_{16} & 0 & 0 \\ G_{63} & G_{61} & G_{61} & G_{66} & 0 & 0 \\ 0 & 0 & 0 & 0 & G_{44} & G_{45} \\ 0 & 0 & 0 & 0 & G_{45} & G_{44} \end{bmatrix},$$

tensor site 4 [Fig. 3(d)]:

$$\begin{bmatrix} G_{33} & G_{31} & G_{31} & -G_{36} & 0 & 0 \\ G_{13} & G_{11} & G_{12} & -G_{16} & 0 & 0 \\ G_{13} & G_{12} & G_{11} & -G_{16} & 0 & 0 \\ -G_{63} & -G_{61} & -G_{61} & G_{66} & 0 & 0 \\ 0 & 0 & 0 & 0 & G_{44} & -G_{45} \\ 0 & 0 & 0 & 0 & -G_{45} & G_{44} \end{bmatrix},$$

tensor site 5 [Fig. 3(e)]:

$$\mathsf{G}^5=\begin{bmatrix} G_{11} & G_{13} & G_{12} & 0 & -G_{16} & 0 \\ G_{31} & G_{33} & G_{31} & 0 & -G_{36} & 0 \\ G_{12} & G_{13} & G_{11} & 0 & -G_{16} & 0 \\ 0 & 0 & 0 & G_{44} & 0 & -G_{45} \\ -G_{61} & -G_{63} & -G_{61} & 0 & G_{66} & 0 \\ 0 & 0 & 0 & -G_{45} & 0 & G_{44} \end{bmatrix},$$

tensor site 6 [Fig. 3(f)]:

$$\mathsf{G}^6=\begin{bmatrix} G_{11} & G_{13} & G_{12} & 0 & G_{16} & 0 \\ G_{31} & G_{33} & G_{31} & 0 & G_{36} & 0 \\ G_{12} & G_{13} & G_{11} & 0 & G_{16} & 0 \\ 0 & 0 & 0 & G_{44} & 0 & G_{45} \\ G_{61} & G_{63} & G_{61} & 0 & G_{66} & 0 \\ 0 & 0 & 0 & G_{45} & 0 & G_{44} \end{bmatrix}.$$